Boundary conditions for acoustic and elastic wave propagation using deep learning

Harpreet Kaur, Sergey Fomel, and Nam Pham, The University of Texas at Austin*

SUMMARY

We propose a deep learning framework to simulate the effect of boundary conditions for wave propagation in anisotropic media. To overcome the challenges associated with stability of conventional implementation of boundary conditions for strongly anisotropic media, we propose an efficient algorithm using deep neural networks. We train the network using a few shot locations and time-slices enabling the network to learn how to remove boundary reflections and simulate wave propagation for unbounded media. The benefit of this approach is its simple implementation and significant reduction of reflections at the boundaries, especially, in the case of tilted transverse isotropic media. We validate the proposed approach by comparing wave propagation at the boundaries using the proposed algorithm with the output obtained using the unbounded media simulated by padding the model. Tests on different models with acoustic and elastic wave propagation verify the effectiveness of the proposed approach.

INTRODUCTION

Given the finite nature of computational memory, a numerical solution for wave propagation can be obtained only at a finite number of points. Therefore, unbounded domains of the wave equation require truncation by introducing boundaries to obtain finite models (Reynolds, 1978; Ionescu and Igel, 2003). The introduction of boundaries in models leads to reflections and wraparound while ideally the wave should propagate through the boundaries with no reflections (Reynolds, 1978). The eventual inward propagation of spurious reflections from the edge of a computational grid masks the true solution for the numerical wave propagation in an infinite media (Clayton and Engquist, 1977). To minimize spurious boundary reflections, boundary conditions must be implemented to avoid numerical instabilities by making the grid boundaries transparent to outward-moving waves (Clayton and Engquist, 1977; Ionescu and Igel, 2003). The conditions need to be such that the solution after implementing the boundary conditions remain as close as possible to the solution obtained using the original physical infinite domain (Nataf, 2013).

Several authors have proposed different sets of boundary conditions for acoustic and elastic media. Engquist and Majda (1977), Clayton and Engquist (1977), and Toldi and Hale (1982) proposed absorbing boundary conditions (ABCs) on the basis of paraxial approximations to model outward-moving energy to reduce reflections from the boundaries. Israeli and Orszag (1981) proposed absorbing boundary conditions with damping using sponge filters. Berenger (1994, 1996) proposed a perfectly matched later (PML) formulation, which is an absorbing region that can provide reflections that are magnitude lower (Nataf, 2013). Implementation of low-reflecting boundary conditions onto open boundaries in the anisotropic models is a challenging problem (Bécache et al., 2003; Appelö and Kreiss, 2006; Sofronov and Zaitsev, 2008). Lower order ABCs are easy to implement; however, they are not accurate in anisotropic cases because they generate spurious reflections. Higher order ABCs are accurate, but their implementation is complicated, and they significantly increase computational cost. PMLs, on the other hand, are easier to implement and have a lower computational cost than ABCs; however, they are unstable for different classes of anisotropic media, especially tilted transverse isotropic (TTI) media (Bécache et al., 2003; Boillot et al., 2012).

In this work, we propose a novel workflow to implement boundary conditions using a deep learning framework. We train the network using a few shot locations and time slices to learn a mapping between the bounded model with boundary reflections and the model with expanded boundaries to simulate the effects of boundary conditions. Once the network learns to attenuate the boundary reflections and wrap around events, we test the proposed approach using different shot locations and time slices of different models that are not a part of training. Using numerical models of increasing complexity, we demonstrate that the proposed approach can effectively simulate the physical behavior of unbounded media for both acoustic and elastic wave propagation.

NETWORK ARCHITECTURE AND TRAINING

We implement a deep learning framework using generative adversarial networks (GANs) (Goodfellow et al., 2014). The network consist of two deep neural networks: a generator (G) and a discriminator (D). G samples the input distribution and maps it to the target distribution. The generated distribution, along with real labels, is fed to the D, which attempts to distinguish how close the two distributions are. The two networks improve their respective abilities until the equilibrium point is reached, where the D is no longer able to distinguish between real and synthesized images. In the GAN framework, the D informs G to tweak the synthesized output towards the more realistic target labels. The generator consists of three different blocks, encoder, transformation block, and decoder. D consists of different convolution layers, with the last layer being the decisive layer that outputs the probability of the sample being from the real distribution or the generated distribution. For the given problem statement, the input domain m consist of wave propagation in the bounded model. This model consists of reflections from the boundaries and the target labels n consist of wave propagation in unbounded media simulated by padding the model. The minimax game between the G and the D is represented by Equation 1:

$$\begin{aligned} minmaxV(G,D) = E_{\mathbf{n}\sim\hat{p}_n}[log\mathbf{D}(\mathbf{n})]+ \\ E_{\mathbf{m}\sim\hat{p}_m}[log(1-\mathbf{D}(\mathbf{G}(\mathbf{m})))], \end{aligned} \tag{1}$$

10.1190/segam2021-3580865.1

where V(G,D) represents the objective function, p_m, and p_n represent the probability distribution of source domain and target domain, and $E_{\mathbf{n}\sim\hat{p}_n}$ and $E_{\mathbf{m}\sim\hat{p}_m}$ are the expected values over real and generated instances, respectively.

We train the network with isotropic, transverse isotropic (TI), and tilted transverse isotropic (TTI) models with different source wavelet frequencies using five shot locations (one in the center and four on the corners of the model) and 25 time slices from each model. We use different time slices of the wave propagation in the bounded model with spurious reflections from boundaries as an input to the network, and the target labels are corresponding time slices in a padded model used to simulate the effect of unbounded media. We use 200 epochs for training using an Adam optimizer with a batch size of 4. During the training phase, the network learns to remove the boundary reflections and make the grid perimeter transparent to the outgoing wave propagation as shown in Figure 1. We test the trained network using different time slices and shot locations of the models that are not a part of training.

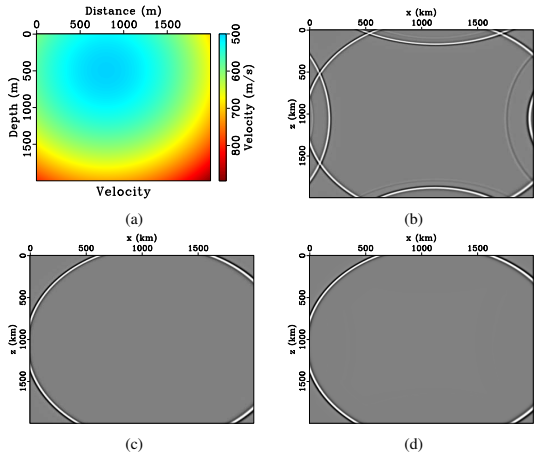

Figure 1: One of the training models with wavefield snapshot at t=2.04 s: (a) gradient velocity model with large velocity variations, (b) wavefield snapshot with boundary reflections, (c) wavefield snapshot without reflections from the boundary in unbounded media simulated by padding the model, and (d) wavefield snapshot using the proposed method. During the training phase, the network learns to attenuate boundary reflections and Fourier wrap arounds. The trained network can then be used to implement boundary conditions on test shots with different models.

EXAMPLES

Marmousi Model

We test the proposed algorithm on the Marmousi model (Versteeg, 1994) using acoustic-wave propagation. The model is based on the North Quenguela trough in the Cuanza basin and is an interesting model for analyzing the complexities in wave propagation (Fomel et al., 2013a). The model is discretized on a 376 $\times$ 384 grid with a spacing of 25 m along vertical and horizontal directions (Kaur et al., 2019b). We simulate the wave propagation using a low-rank extrapolation operator (Fomel et al., 2013b; Sun et al., 2016) with a 15-Hz Ricker wavelet. We test the trained network with different time slices and shot locations that are not a part of training. We input the acoustic wave propagation with boundary reflections as shown in Figure 2a into the network and the network applies boundary conditions to remove reflections from boundaries, as well as Fourier wrap-around and outputs Figure 2b. This output is close to the output of the unbounded media shown in Figure 2c simulated by padding the model. We further test on different blind-test locations that are not a part of training. Figure 2d shows wave propagation with reflections from the boundary for the blind-test-shot location. The network applied boundary conditions and outputs Figure 2e, where boundary reflections and wraparound have been removed and output is close to wave propagation output using unbounded media as shown in Figure 2f.

Two-layer TI model

For the elastic wave-propagation case, we start with a two-layer transverse isotropic model previously used by Cheng and Fomel (2014); Kaur et al. (2019a). The model is discretized on a 400 $\times$ 400 grid. The top layer of the model is the VTI medium with v_{p0}=2500 m/s, v_{s0}=1200 m/s, δ=-0.25, and ϵ=0.25. The bottom layer is a TTI medium with v_{p0}=3600 m/s, v_{s0}=1800 m/s, δ=0.1, and ϵ=0.2 and a tilt of θ=30°. We simulate wave propagation using a 15-Hz Ricker wavelet and low-rank extrapolation operator. We test the trained network with different time slices and source location that are not a part of training. Figure 4a and 4d shows one of the test slices of the horizontal and the vertical components of the wavefield with spurious reflections from the boundaries. The network applies learned weights during the training process to simulate the effect of boundary conditions and output Figure 4b and 4d. The output of the proposed method is close to the output using unbounded media (simulated by padding the bounded media) shown in Figure 4c and 4f.

BP 2007 TTI model

A last example of boundary conditions using elastic wave propagation is the BP 2007 TTI model. We have shown application of the proposed method using a part of the BP 2007 TTI model consisting of salt. The velocity model, along with the Thomsen coefficients, is shown in Figure 3. The model is discretized on a 400 $\times$ 400 grid with a vertical and horizontal spacing of 6.25 m. This example is interesting because the conventional low-order implementation of ABCs and PMLs is challenging for TTI media. In the TTI case, instabilities may appear in layers with PMLs owing to exponentially increasing modes, which eventually degrades the reverse time migration output. Therefore, the proposed algorithm is especially important for TTI cases. We input horizontal and vertical components of the elastic wavefield shown in Figure 5a and 5d with boundary reflections into the network. The trained network applied the boundary conditions and outputs Figure 5b and 5e with removal of reflections from the boundary. The output using the proposed method is close to the reference output using the unbounded media simulated by padding the model as shown in Figure 5c and 5f. We use two different metrics- the structural similarity index (SSIM) and correlation coefficient R^2 (Table

10.1190/segam2021-3580865.1

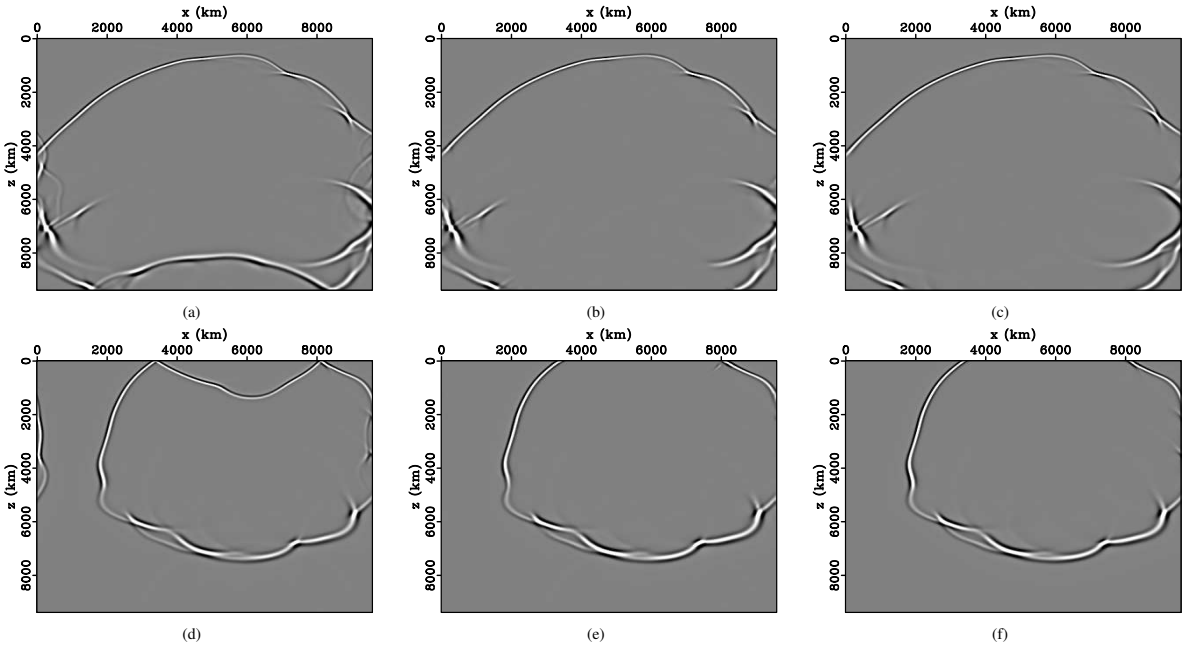

Figure 2: Blind-test dataset for the Marmousi model (these time slices are not a part of training). Wavefield snapshot at t=1.88 s: (a) wavefield snapshot with boundary reflections, (b) wavefield snapshot using the proposed method, and (c) wavefield snapshot without boundary reflections in unbounded media simulated by padding the model. Wavefield snapshot at t=1.96 s for a different blind-test shot location: (a) wavefield snapshot with boundary reflections, (b) wavefield snapshot using the proposed method, and (c) wavefield snapshot without boundary reflections in unbounded media simulated by padding the model.

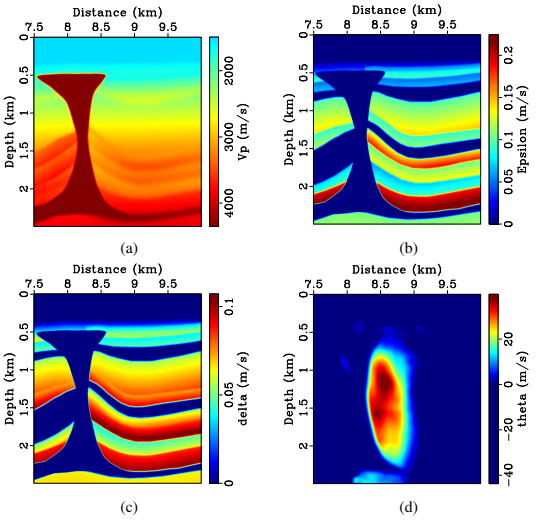

Figure 3: BP 2007 TTI model with (a) vertical P-wave velocity Vp, and Thomsen coefficients (b) ϵ, (c) δ, and (d) tilt-angle *theta*.

1) to show that the output of the proposed algorithm is close to the reference time slices for unbounded media simulated by padding the model.

Table 1: Structural-similarity index and correlation coefficient for different models. Marmousi model output is with acoustic wave propagation; therefore, U_x and U_z are similar in the table.

Models	U_x(SSIM)	$U_x(R^2)$	U_z(SSIM)	$U_z(R^2)$
Marmousi	0.999	0.962	0.999	0.962
Two-layer TI	0.985	0.995	0.989	0.997
BP TTI	0.981	0.995	0.985	0.995

CONCLUSIONS

We have developed a deep neural network based workflow for application of boundary conditions during wave propagation in anisotropic media. The idea is to train the network with a few shot locations and time slices such that the network learns to attenuate boundary reflections and Fourier wraparounds on model boundaries. The trained network can then be applied to test shots with different models that are not a part of training. The proposed approach is stable and simulates the effect of higher order absorbing boundary conditions at a fraction of the cost of conventional implementation in strongly anisotropic media especially, TTI media, thus having a great potential for application in reverse time migration.

10.1190/segam2021-3580865.1

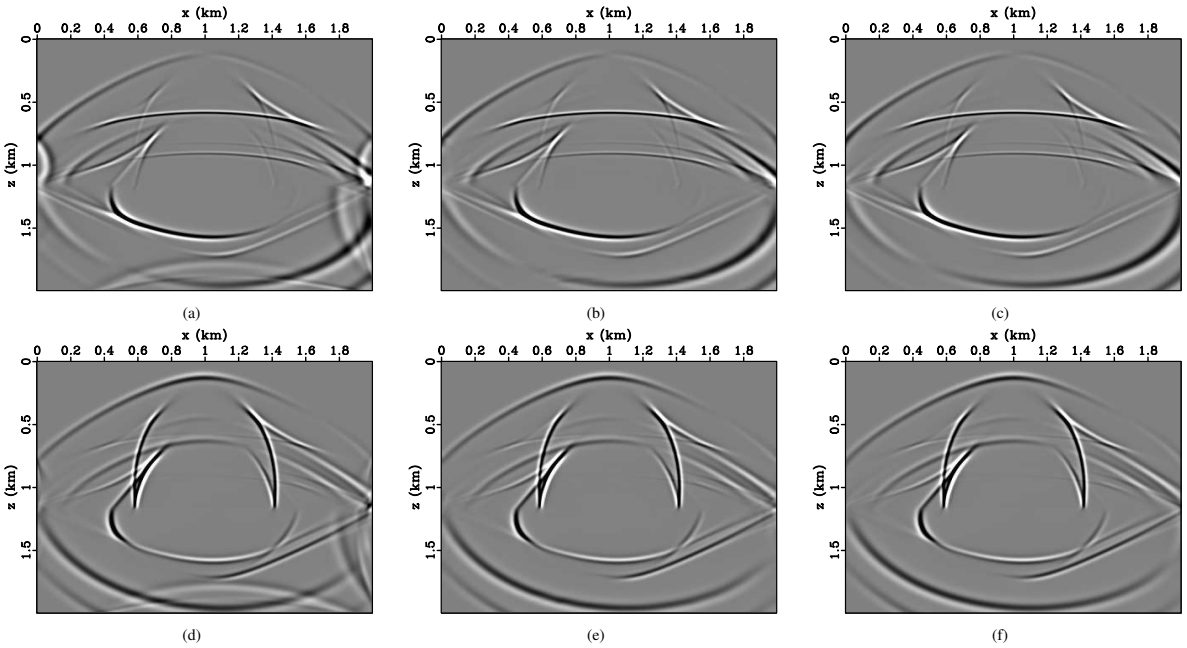

Figure 4: Blind-test dataset for two-layer TI model, with wavefield snapshot at t=0.39 s. Horizontal and vertical components of seismic wavefield: (a) and (d) with boundary reflections, (b) and (e) reflections from boundaries removed using the proposed method, and (c) and (f) reflections in unbounded media simulated by padding the model.

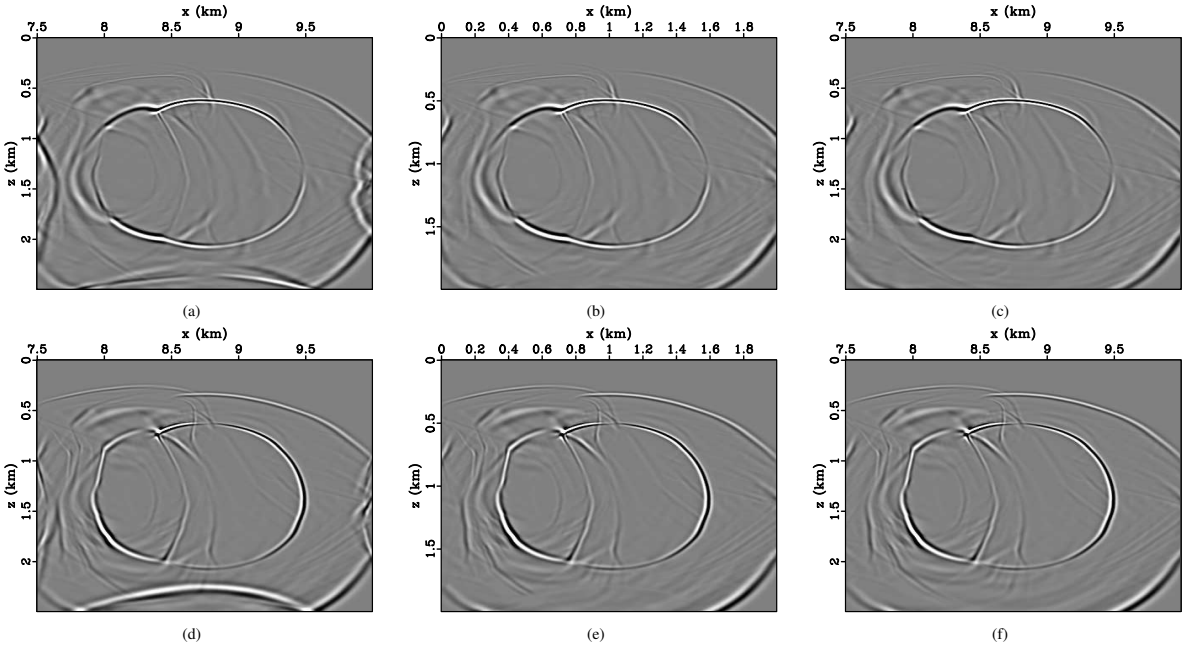

Figure 5: Blind-test dataset for BP 2007 TTI model, with wavefield snapshot at t=0.46 s. Horizontal and vertical components of seismic wavefield: (a) and (d) with boundary reflections, (b) and (e) reflections from boundaries removed using the proposed method, and (c) and (f) reflections in unbounded media simulated by padding the model.

10.1190/segam2021-3580865.1

REFERENCES

Appelo, D., and G. Kreiss, 2006, A new absorbing layer for elastic waves: Journal of Computational Physics, **215**, 642–660, doi: https://doi.org/10.1016/j.jcp.2005.11.006.

Becache, E., S. Fauqueux, and P. Joly, 2003, Stability of perfectly matched layers, group velocities and anisotropic waves: Journal of Computational Physics, **188**, 399–433, doi: https://doi.org/10.1016/S0021-9991(03)00184-0.

Berenger, J.-P., 1994, A perfectly matched layer for the absorption of electromagnetic waves: Journal of Computational Physics, **114**, 185–200. doi: https://doi.org/10.1006/jcph.1994.1159.

Berenger, J.-P., 1996, Three-dimensional perfectly matched layer for the absorption of electromagnetic waves: Journal of Computational Physics, **127**, 363–379. doi: https://doi.org/10.1006/jcph.1996.0181.

Boillot, L., H. Barucq, H. Calandra, and J. Diaz, 2012, Absorbing boundary conditions for anisotropic elastodynamic media: HOSCAR-1st Brazil-French Workshop on High Performance Computing and Scientific Data Management Driven by Highly Demanding Applications (INRIA-CNPQ).

Cheng, J., and S. Fomel, 2014, Fast algorithms for elastic-wave-mode separation and vector decomposition using low-rank approx-imation for anisotropic media: Geophysics, **79**, C97–C110, doi: https://doi.org/10.1190/geo2014-0032.1.

Clayton, R., and B. Engquist, 1977, Absorbing boundary conditions for acoustic and elastic wave equations: Bulletin of the Seismological Society of America, **67**, 1529–1540.

Engquist, B., and A. Majda, 1977, Absorbing boundary conditions for numerical simulation of waves: Proceedings of the National Academy of Sciences, **74**, 1765–1766. doi: https://doi.org/10.1073/pnas.74.5.1765.

Fomel, S., L. Ying, and X. Song, 2013b, Seismic wave extrapolation using lowrank symbol approximation: Geophysical Prospecting, **61**, 526–536. doi: https://doi.org/10.1111/j.1365-2478.2012.01064.x.

Fomel, S., P. Sava, I. Vlad, Y. Liu, and V. Bashkardin, 2013a, Madagascar: Open-source software project for multidimensional data analysis and reproducible computational experiments: Journal of Open Research Software, **1**, e8. doi: https://doi.org/10.5334/jors.ag.

Goodfellow, I., J. Pouget-Abadie, M. Mirza, B. Xu, D. Warde-Farley, S. Ozair, A. Courville, and Y. Bengio, 2014, Generative adversarial nets: Advances in Neural Information Processing Systems, 2672–2680.

Ionescu, D.-C., and H. Igel, 2003, Transparent boundary conditions for wave propagation on unbounded domains: International Conference on Computational Science, 807–816.

Israeli, M., and S. A. Orszag, 1981, Approximation of radiation boundary conditions: Journal of Computational Physics, **41**, 115–135. doi: https://doi.org/10.1016/0021-9991(81)90082-6.

Kaur, H., S. Fomel, and N. Pham, 2019a, Elastic wave-mode separation in heterogeneous anisotropic media using deep learning: 89th Annual International Meeting, SEG, Expanded Abstracts, 2654–2658, doi: https://doi.org/10.1190/segam2019-3207506.1.

Kaur, H., S. Fomel, and N. Pham, 2019b, Overcoming numerical dispersion of finite-difference wave extrapolation using deep learning: 89th Annual International Meeting, SEG, Expanded Abstracts, 2318–2322, doi: https://doi.org/10.1190/segam2019-3207486.1.

Nataf, F., 2013, Absorbing boundary conditions and perfectly matched layers in wave propagation problems.

Reynolds, A. C., 1978, Boundary conditions for the numerical solution of wave propagation problems: Geophysics, **43**, 1099–1110. doi: https://doi.org/10.1190/1.1440881.

Sofronov, I. L., and N. A. Zaitsev, 2008, Transparent boundary conditions for the elastic waves in anisotropic media: *in* Hyperbolic Problems: Theory, Numerics, Applications: Springer, 997–1004.

Sun, J., S. Fomel, and L. Ying, 2016, Low-rank one-step wave extrapolation for reverse time migration: Geophysics, **81**, no. 1, S39–S54. doi: https://doi.org/10.1190/geo2015-0183.1.

Toldi, J., and I. D. Hale, 1982, Data-dependent absorbing boundaries: SEP-30: Stanford Exploration Project, 111–120.

Versteeg, R., 1994, The marmousi experience: Velocity model determination on a synthetic complex data set: The Leading Edge, **13**, 927–936. doi: https://doi.org/10.1190/1.1437051.